ARMY RESEARCH LABORATORY

Plate-Impact Measurements of a Select Model Poly(urethane urea) Elastomer

by Daniel T. Casem and Alex J. Hsieh

ARL-TR-6482 June 2013

NOTICES

Disclaimers

The findings in this report are not to be construed as an official Department of the Army position unless so designated by other authorized documents.

Citation of manufacturer's or trade names does not constitute an official endorsement or approval of the use thereof.

Destroy this report when it is no longer needed. Do not return it to the originator.

Army Research Laboratory
Aberdeen Proving Ground, MD 21005-5069

ARL-TR-6482 **June 2013**

Plate-Impact Measurements of a Select Model Poly(urethane urea) Elastomer

Daniel T. Casem and Alex J. Hsieh
Weapons and Materials Research Directorate, ARL

REPORT DOCUMENTATION PAGE	Form Approved OMB No. 0704-0188

1. REPORT DATE *(DD-MM-YYYY)*	2. REPORT TYPE	3. DATES COVERED (From - To)
June 2013	Final	1 September 2011–31 August 2012

4. TITLE AND SUBTITLE	5a. CONTRACT NUMBER
Plate-Impact Measurements of a Select Model Poly(urethane urea) Elastomer	5b. GRANT NUMBER
	5c. PROGRAM ELEMENT NUMBER
6. AUTHOR(S)	5d. PROJECT NUMBER
Daniel T. Casem and Alex J. Hsieh	5e. TASK NUMBER
	5f. WORK UNIT NUMBER
7. PERFORMING ORGANIZATION NAME(S) AND ADDRESS(ES)	8. PERFORMING ORGANIZATION REPORT NUMBER
U.S. Army Research Laboratory ATTN: RDRL-WMM-G Aberdeen Proving Ground, MD 21005-5069	ARL-TR-6482
9. SPONSORING/MONITORING AGENCY NAME(S) AND ADDRESS(ES)	10. SPONSOR/MONITOR'S ACRONYM(S)
	11. SPONSOR/MONITOR'S REPORT NUMBER(S)

12. DISTRIBUTION/AVAILABILITY STATEMENT

Approved for public release; distribution is unlimited.

13. SUPPLEMENTARY NOTES

14. ABSTRACT

Plate-impact experiments were conducted to highlight the high-pressure, high-strain-rate response of a select model poly(urethane urea) (PUU) elastomer impacted against stationary soda lime glass target plates. The dynamic stress-strain behavior reveals that the stress level reaches 0.672 and 3.042 GPa at impact velocities of 298 and 998 m/s, respectively. The PUU is partially unloaded in four successive steps after the initial compression at the impact velocity of 298 m/s and three successive steps at 998 m/s. Thus, data is obtained along the Hugoniot and along the release path. The release path and the Hugoniot coincide over the range of pressures studied.

15. SUBJECT TERMS

plate impact, poly(urethane urea), elastomer, high strain rate, high-pressure deformation

16. SECURITY CLASSIFICATION OF:			17. LIMITATION OF ABSTRACT	18. NUMBER OF PAGES	19a. NAME OF RESPONSIBLE PERSON
a. REPORT	b. ABSTRACT	c. THIS PAGE			Daniel T. Casem
Unclassified	Unclassified	Unclassified	UU	16	19b. TELEPHONE NUMBER (*Include area code*) 410-306-0698

Standard Form 298 (Rev. 8/98)
Prescribed by ANSI Std. Z39.18

Contents

List of Figures

List of Tables

1. Introduction

High-performance polyurea elastomers have recently gained considerable interest throughout the U.S. Department of Defense (DOD), particularly for their potential in ballistic impact protection and blast mitigation capabilities (*1–6*). There have been extensive studies on high-strain-rate mechanical deformation and modeling (*3*, *6–11*), wherein most are focused on a commercial polyurea. The commercial polyureas that are of interest to DOD are typically a two-component system, yet the majority of research and development on polyurethane, poly(urethane urea), and polyurea elastomers has been based on a three-component system (*12–18*) for use in a broad range of applications (*19*). These elastomers are known to have versatile chemistry yet complex microstructure.

Recent studies of select model 4,4'-dicyclohexylmethane diisocyanate (HMDI)−poly (tetramethylene oxide) (PTMO)–diethyltoluenediamine (DETA)-based poly(urethane urea) (PUU) elastomers have demonstrated the composition dependence of tunable microstructure (*20–25*) as well as the microstructure evolution (*24*, *25*). These PUUs consist of an aliphatic 4,4'-dicyclohexylmethane diisocyanate, which is much more flexible in terms of chain conformation than an aromatic 4,4'-diphenylmethane diisocyanate (MDI) used in the commercial polyureas. Altering the molecular weight (MW) of the PTMO soft segment (SS) while keeping the molar ratio of HMDI:PTMO:DETA constant (2:1:1) causes a drastic change in microstructure. At SS MW 2000 g/mol, spherulite-like hard domains were observed within a SS-rich matrix via atomic force microscopy (AFM) phase images (*23–25*), whereas greater phase mixing between the hard and soft segment was evidenced as the SS MW decreased. For a SS MW of 1000 g/mol there was a coexistence of lamellar hard segment domains dispersed in a matrix consisting of a fibrillar-like microstructure (*23–25*), whereas an almost featureless microstructure was noted in PUU with SS MW 650 g/mol (*25*). These AFM observations were shown to be consistent with small-angle x-ray scattering results and dynamic mechanical analysis (DMA) loss tangent data. Correspondingly, an increase in SS glass transition temperature (T_g) and a broadening of the SS relaxation were noted in PUUs with decreasing SS MW based on the DMA data (*20–22*, *25*). Additionally, greater strain-rate sensitivity upon dynamic mechanical deformation was also evidenced with respect to better phase mixing (*20–22*).

Bogoslovov et al. (*3*) have proposed that deformation-induced glass transition is a plausible molecular mechanism responsible for the performance enhancement in polyurea in addition to other potential mechanisms such as shock impedance mismatch, shock-wave dispersion, and strain delocalization. Under high-rate loading conditions, the physical response of this class of material can be tailored to transition from a rubbery-like to a leathery-like or a glassy state with increasing strain rate, where stress levels may be greatly enhanced and large energy-dissipation

mechanisms can be realized (*3*). Additionally, the polyurea coating when subjected to impact was also reported to experience a locally elevated pressure, in addition to the compressive strain (*26*). There have been studies addressing the pressure-sensitivity including pressure-shear plate impact measurements of a polyurea elastomer at very high strain rates, $10^5 – 10^6 s^{-1}$ (*27–29*). Results showed that shearing resistance of polyurea was significantly dependent upon pressure. Our research objective is to better understand the molecular influence on viscoelastic response of PUUs, particularly under high strain rate and high-pressure loading conditions. In this work, we exploit plate impact measurements and report the preliminary experimental findings on high pressure response obtained for a select model PUU.

2. Experimental

2.1 Materials

A select model PUU composed of 4,4'-dicyclohexylmethane diisocyanate (HMDI – Desmodur W, Bayer MaterialScience), diethyltoluenediamine (DETA – Ethacure* 100-LC, Albemarle Corporation, Baton Rouge, Louisiana), and poly(tetramethylene oxide) (PTMO – PolyTHF, BASF Corporation) was chosen for this study. This PUU was prepared using a two-step pre-polymer synthesis method; details of the synthesis can be found in Sarva et al. (*20*). Typically, PTMO, the soft segment, was first reacted with HMDI to form a pre-polymer with a urethane linkage, and the reaction was carried out to ensure PTMO was completely end-capped with diisocyanate groups. The pre-polymer was then reacted with the chain extender, DETA, to complete polymerization. The reaction of HMDI with the DETA diamine resulted in hard segments with urea linkages, which could self-assemble to form domains and thus leading to microphase separation. The as-cast sheets were fabricated using an in situ polymerization/cast approach (*20*).

The PUU composition of interest has a molar ratio 5:3:2 of diisocyanate:diamine chain extender:PTMO, where the MW of PTMO is 1000 g/mol. The hard segment content (HS_u) used in this work only accounts for the portion of diisocyanate that reacts with diamine and is calculated to be about 34% according to the following equation (*18*).

$$\%HS_u = \frac{100(R-1)(M_{di}+M_{da})}{(M_g + R(M_{di}) + (R-1)(M_{da}))}. \quad (1)$$

*Ethacure is a registered trademark of Albemarle Corporation, Baton Rouge, LA.

2.2 Plate Impact

Plate-impact experiments were conducted to gain insight into the high-pressure response of PUU. Two experiments were conducted in the configuration shown in figure 1. The PUU specimens were disk-shaped, nominally 3.4 mm in thickness and 40 mm in diameter. They were accelerated in a light gas gun and impacted against stationary soda lime glass target plates (nominally 2.0 mm thick, 40-mm diameter) at impact speeds of 298 and 998 m/s. The impact velocities are such that the soda lime glass remains elastic throughout the experiments. The particle velocities at the center of the free surface of the target plates were monitored with a Velocity Interferometer System for Any Reflector (VISAR) (*30*). These measurements are accurate to within +/–1% and have a 0.5-ns time resolution. Impact speeds are measured just prior to impact with a series of electrically conducting pins, to an accuracy of +/–1%.

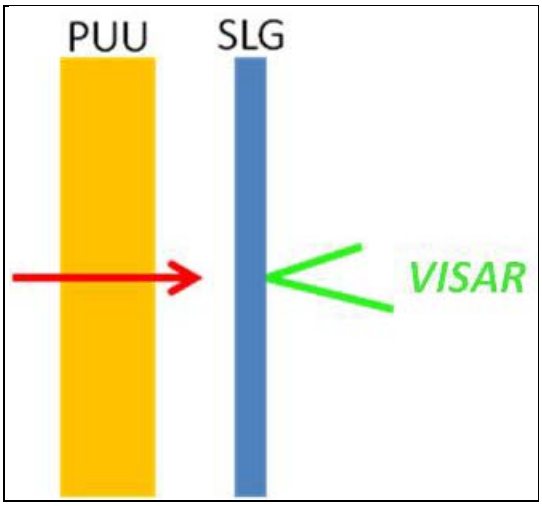

Figure 1. A schematic of shot configuration used in plate impact measurements of PUU against stationary soda lime glass (SLG) target.

The basic concept of the plate impact experiment is to use the measured behavior of the soda lime glass along with its known properties to infer the behavior of the PUU flyer. The impact produces shock waves that transmit into both the flyer and the target. The dimensions are such that one dimensional strain conditions are maintained for all relevant data.

3. Results and Discussion

For plate-impact measurements, a Lagrangian x-t diagram reflecting the target position-time profile can be generated. This diagram is shown in figure 2 for the 298 m/s experiment. The release wave from the free-surface of the PUU arrives at the measurement point approximately 3 μs after impact; this ends the test. However, the soda lime glass is thin enough such that several reverberations occur during this time. Each reverberation causes the stress to release, i.e., the PUU is partially unloaded in four successive steps after the initial compression.

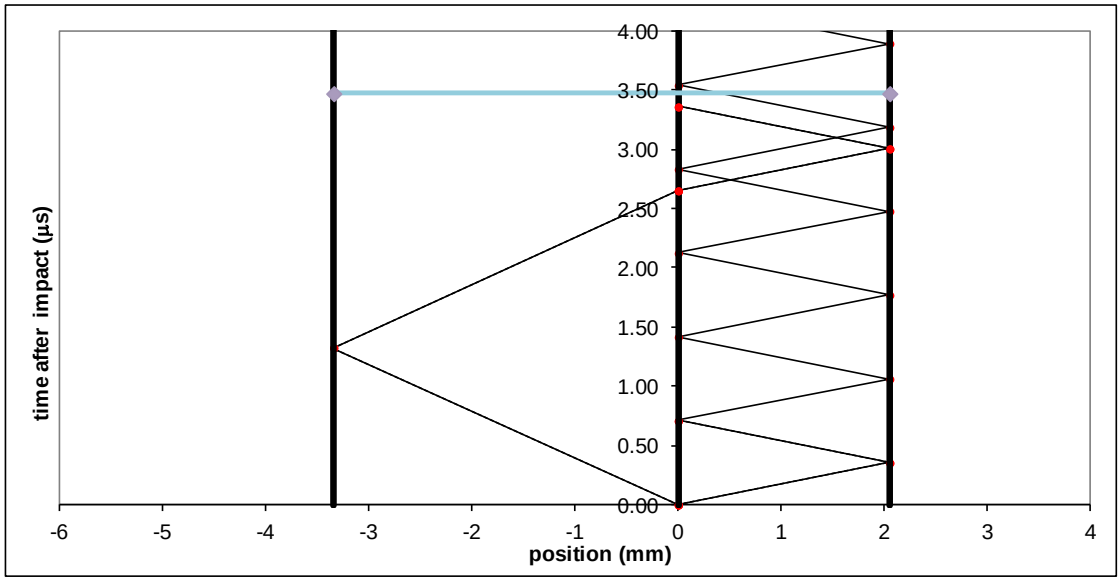

Figure 2. A Lagrangian x-t diagram for the shock experiment at 298 m/s.

The measured velocity for the 298 m/s experiment is shown in figure 3. The steps in the velocity profile are easily discerned. To reiterate, as each reflection reaches the interface between the sample and the target, the stress is released, resulting in a step-increase in the free-surface particle velocity. As previously noted, the soda lime glass remains elastic, with properties of density $\rho = 2.49$ kg/m^3 and longitudinal wave velocity $c_L = 5.79$ m/s. The free-surface velocities, u_{free}, are estimated from the figure and listed for each state in table 1; $i = 1$ denotes the initial shock, and $i = 2$, 3 and 4 the three release states.

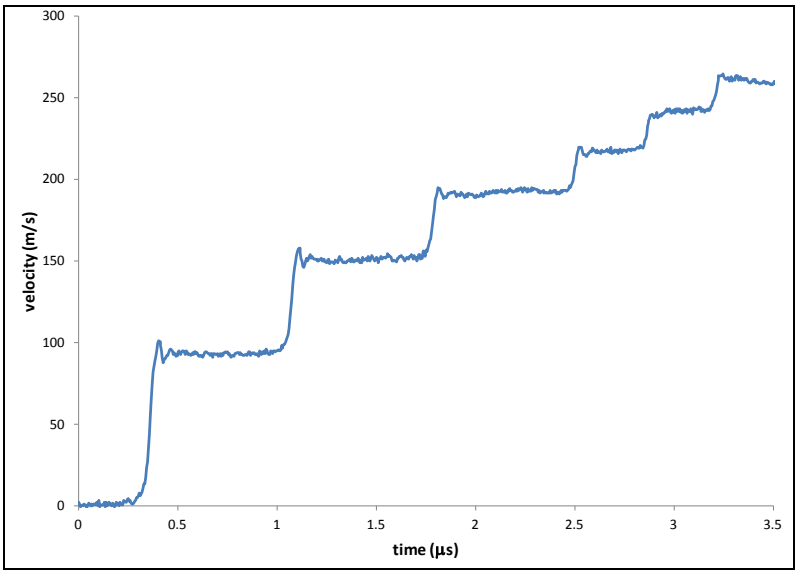

Figure 3. Free-surface velocity of soda lime glass for the plat-impact experiment at 298 m/s.

The stresses, σ_i, are calculated from the particle velocity using the known elastic impedance of the glass. These stresses act on both target and flyer. Since the impact speed is known, particle velocity within the PUU, in the reference frame of the moving projectile, can be calculated. These are listed in table 1, u_i and ρ_i are used along with the stresses to calculate the shock speeds $Us,_i$ using the Hugoniot momentum equation:

$$U_{i+1} = u_i + \frac{1}{\rho_i}\left(\frac{\sigma_{i+1} - \sigma_i}{u_{i+1} - u_i}\right). \tag{2}$$

The mass equation is used to determine density, ρ_i, for each state.

$$\rho_{i+1} = \rho_i\left(\frac{U_{i+1} - u_i}{U_{i+1} - u_{i+1}}\right). \tag{3}$$

The compressive engineering strain can be found from the initial density, ρ_0, by

$$\varepsilon_i = 1 - \frac{\rho_0}{\rho_i}, \tag{4}$$

since one-dimensional strain conditions are maintained. U_P refers to the particle velocity due to the shock in the PUU. The velocity from the initial step is a point on the Hugoniot and is determined from the measured velocity using the following:

$$U_{P,1} = V_0 - \frac{u_1}{2}. \tag{5}$$

Particle velocity associated from the release steps can be determined similarly (i = 2, 3, . . .).

$$U_{P,i} = V_0 - \frac{u_i + u_{i+1}}{2}. \quad (6)$$

Here, V_0 is the impact speed. These quantities are also reported in table 1.

Table 1. Data including density, stress, strain, particle velocity, and shock speed obtained for the 298 m/s experiment.

Step No.	Density (kg/m^3)	Strain	Stress (GPa)	U_S (m/s)	U_P (m/s)
0	1061	0	0.000	NA	0
1	1179	0.099812	0.672	2519	251
2	1148	0.076111	0.417	3119	176
3	1124	0.056339	0.288	2461	127
4	1110	0.043767	0.194	2638	94

For the 998 m/s experiment, the PUU is partially unloaded in three successive steps after the initial compression. The values of u_{free} estimated from the initial shock and two release states are listed in table 2. The response of the PUU, in terms of stress versus strain, is shown in figure 4, wherein at each impact velocity the highest stress point is on the Hugoniot. The stress-strain data along the release path appear to coincide with those on the Hugonoit obtained for both the 298 and 998 m/s experiments.

Table 2. Data including density, stress, strain, particle velocity, and shock speed obtained for the 998 m/s experiment.

Step No.	Density (kg/m^3)	Strain	Stress (GPa)	U_S (m/s)	U_P (m/s)
0	1061	0	0.000	NA	0
1	1353	0.216025	3.042	3643	787
2	1249	0.150392	1.463	4520	475
3	1192	0.109566	0.815	3763	317

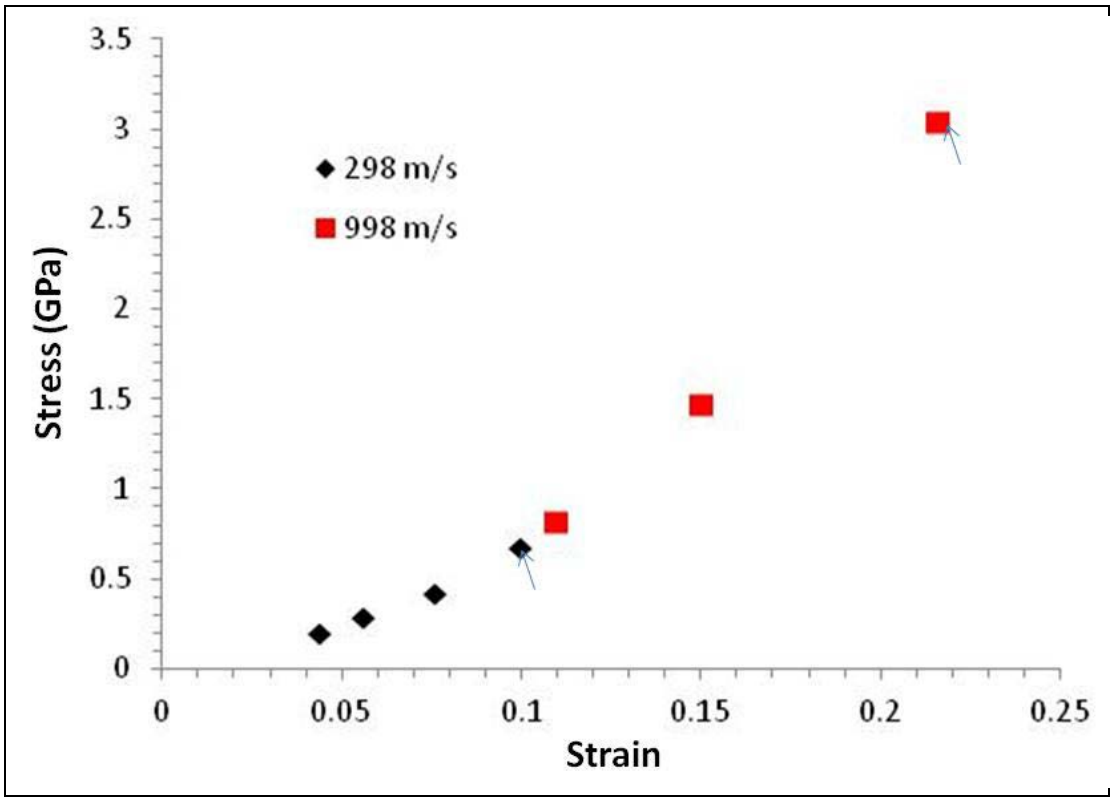

Figure 4. Stress-strain behavior of PUU obtained from plate impact measurements (arrows pointing to data on the Hugoniot).

Although most of the data in figure 4 is for release behavior, an attempt was made to generate a correlation of shock velocity (Us) vs. particle velocity (Up) for the data that represent the highest stress point on the Hugoniot from each experiment. This is shown in figure 5, along with the Us-Up obtained for polyurea by Casem et al. (*31*) for comparison. These preliminary results indicate that the plate impact behavior of the select model PUU appears to be very similar to those of the commercial polyurea at velocity in the range of 298–1000 m/s, despite their difference in terms of molecular structure.

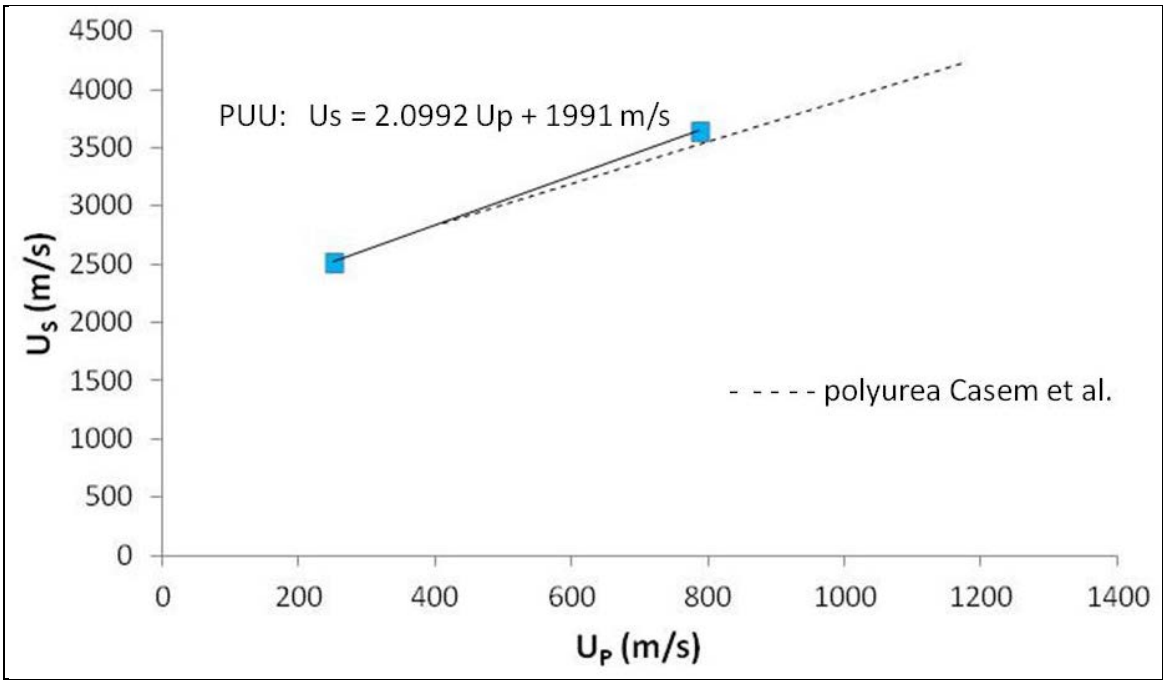

Figure 5. Plot of Us-Up for PUU, based on the Hugoniot states measured in two experiments, and data for polyurea (dashed line) (*31*) are also included for comparison.

Further plate-impact measurements are in progress, particularly with an attempt for determination of an equation of state (EOS) for this PUU. The latter is of interest for the multiscale modeling for validation of EOS.

4. Conclusion

Plate-impact measurements of a select model PUU elastomer have been made. Longitudinal stresses of 0.672 and 3.042 GPa are achieved at impact velocities of 298 and 998 m/s, respectively. For the 298 m/s experiment, the PUU is partially unloaded in four successive steps after the initial compression, while three successive steps of unloading occur in the 998 m/s experiment. Additionally, the data obtained for the Hugoniot state appear to coincide with those obtained along the release path from both experiments. Measurements of Us vs. Up also show that the Hugoniot of this material is similar to that of polyurea.

5. References

1. Porter, J. R.; Dinan, R. J.; Hammons, M. I.; Knox, K. J. Polymer Coatings Increase Blast Resistance of Existing and Temporary Structures; *AMPTIAC Quart.* **2002**, *6*, 47.
2. Davidson, J. S.; Fisher, J. W.; Hammons, M. I.; Porter, J. R.; Dinan, R. J. Failure Mechanisms of Polymer-Reinforced Concrete Masonry Walls Subjected to Blast; *J. Struct. Eng*. **2005**, *131*, 1194-1205.
3. Bogoslovov, R. B.; Roland, C. M.; Gamache, R. Impact-induced Glass Transition in Elastomeric Coatings; *Appl. Phys. Lett*. **2007**, *90*, 221910–221910-3.
4. Bahei-El-Din, Y. A.; Dvorak, G. J.; Fredricksen, O. J. A Blast-tolerant Sandwich Plate Design with a Polyuera Interlayer; *Int'l J. Solid Structures* **2006**, *43*, 7644.
5. Tekalur, S. A.; Shukla, A.; Shivakumar, K. Blast Resistance of Polyurea-based Layered Composite Materials; *Composite Structures* **2008**, *84*, 271.
6. Roland, C.; Fragiadakis, D.; Gamache, R. Elastomer-steel Laminate Armor; *Composite Structures* **2009**, *92*, 1059–1064.
7. Yi, J.; Boyce, M. C.; Lee, G. F.; Balizer, E. Large Deformation Rate-dependent Stress-strain Behavior of Polyurea and Polyurethanes; *Polymer* **2006**, *47*, 319–329.
8. Sarva, S.; Deschanel, S.; Boyce, M. C.; Chen, W. Stress—strain Behavior of a Polyurea and a Polyurethane from Low to High Strain Rates; *Polymer* **2007**, *48*, 2208–2213.
9. Fragiadakis, D.; Gamache, R.; Bogoslovov, R. B.; Roland, C. M. Segmental Dynamics of Polyurea: Effect of Stoichiometry; *Polymer* **2010**, *51*, 178–184.
10. Grujicic, M.; Pandurangan, B.; He, T.; Cheeseman, B. A.; Yen, C-F.; Randow, C. L. Computational Investigation of Impact Energy Absorption Capability of Polyurea Coating via Deformation-induced Glass Transition; *Materials Science and Engineering A* **2010**, *527*, 7741–7751.
11. Grujicic, M.; Pandurangan, B.; King, A. E.; Runt, J.; Tarter, J.; Dillon, G. J. Multi-length Scale Modeling and Analysis of Microstructure Evolution and Mechanical Properties in Polyurea; *Mater. Sci*. **2011**, *46*, 1767–1779.
12. Wang, C. B.; Cooper, S. L. Morphology and Properties of Segmented Polyether Polyurethaneureas; *Macromolecules* **1983**, *16*, 775–786.
13. Koevoets, R. A.; Versteegen, R. M.; Kooijman, H.; Spek, A. L.; Meijer, E. W. Molecular Recognition in a Thermoplastic Elastomer; *J. Am Chem. Soc*. **2005**, *127*, 2999–3003.

14. Kojio, K.; Furukawa, M.; Motokucho, S.; Shimada, M.; Sakai, M. Structure-Mechanical Property Relationships for Poly(carbonate urethane) Elastomers with Novel Soft Segments; *Macromolecules* **2009**, *42*, 8322–8327.

15. Yilgor, E.; Isik, M.; Yilgor, I. Novel Synthetic Approach for the Preparation of Poly(urethaneurea) Elastomers; *Macromolecules* **2010**, *43*, 8588–8593.

16. Korley, L. T. J.; Pate, B. D.; Thomas, E. L.; Hammond, P. T. Effect of the Degree of Soft and Hard Segment Ordering on the Morphology and Mechanical Behavior of Semicrystalline Segmented Polyurethanes; *Polymer* **2006**, 47, 3073–3082.

17. Sheth, J. P.; Unal, S.; Yilgor, E.; Yilgor, I.; Beyer, F. L.; Long, T. E.; Wilkes, G. L. Comparative Study of the Structure-Property Behavior of Highly Branched Segmented Poly(urethane urea) Copolymers and their Linear Analogs; *Polymer* **2005**, *46*, 10180–10190.

18. O'Sickey, M. J.; Lawrey, B. D.; Wilkes, G. L. Structure-Property Relationships of Poly(urethane urea)s with Ultra-low Monol Content Poly(propylene Glycol) Soft Segments – Influence of Soft Segment Molecular Weight and Hard Segment Content; *J. Appl. Poly. Sci*. **2002**, *84*, 229–243.

19. Holden, G.; Legge, N.; Quirk, R.; Schroeder, H. *Thermoplastic Elastomers*, 2nd ed.; Hanser Publishers: Munich, Germany, 1996.

20. Sarva, S.; Hsieh, A. J. The Effect of Microstructure on the Rate-dependent Stress-Strain Behavior of Poly(urethane urea) Elastomers, *Polymer* **2009**, *50*, 3007–3015.

21. Rinaldi, R.; Hsieh, A. J.; Boyce, M. C. Tunable Microstructures and Mechanical Deformation in Transparent Poly(urethane urea)s; *J. Polym. Sci. Polym. Phys*. **2011**, *49*, 123–135.

22. Hsieh, A. J.; Yu, J. H.; Rinaldi, R.; Krogman, K. C.; Hammond, P. T.; Boyce, M. C; Rice, N. Poly(urethane urea)s with Tunable Microstructures – From Robust Mechanical Strengthening to Chemical Hardening; *Proc. 27th Army Science Conference*, Orlando, FL, 2010.

23. Hsieh, A. J.; Strawhecker, K. E. Microstructure Analysis of Transparent Poly(urethane urea) Elastomers via AFM; *PMSE Preprints of the American Chemical Society*, Vol. *105*, American Chemical Society: Denver, CO, 2011; pp 162–163.

24. Chantawansri, T. L.; Hsieh, A. J. *Hierarchical Elastomers with Tunable Microstructures: Molecular Modeling from Robust Mechanical Strengthening to Multi-functionalities (Final Report);* ARL-TR-6369, U.S. Army Research Laboratory: Aberdeen Proving Ground, MD, 2013.

25. Strawhecker, K. E.; Hsieh, A. J.; Chantawansri, T. L.; Kalcioglu, Z. I.; Van Vliet, K. J. Influence of Microstructure on Micro-/Nano-mechanical Measurements of Select Model Transparent Poly(urethane urea) Elastomers; *Polymer*, **2013**, *54*, 901–908.

26. Roland, C. M.; Casalini, R. Effect of Hydrostatic Pressure on the Viscoelastic Response of Polyurea; *Polymer* **2007**, *48*, 5747–5752.

27. Jiao, T.; Clifton, R. J.; Grunschel, S. E. Pressure-Sensitivity and Constitutive Modeling of AN Elastomer at High Strain Rates; *Shock Compression of Condensed Matter 2009: Proceedings of the American Physical Society Topical Group on Shock Compression of Condensed Matter; American Institute of Physics Conference Proceedings,* **2009**, *1195*, 1229–1232.

28. Chakkarapani, V.; Liechti, K. M.; Ravi-Chandar, K. Characterization of Multiaxial Constitutive Properties of Rubbery Polymers; *J. Eng. Mater. Tech.* **2006**, *128*, 489–496.

29. Chevellard, G.; Ravi-Chandar, K.; Liechti, K. M. Modeling the Nonlinear Viscoelastic Behavior of Polyurea Using a Distortion Modified Free Volume Approach; *Mech. Time-Depend. Mater*. **2012**, *16*, 181–203.

30. Barker, L. M.; Hollenbach, R. E. Laser Interferometer for Measuring High Velocities of Any Reflecting Surface. *J. Appl. Phys.* **1972**, *43* (11), 4669–4675.

31. Casem, D. T.; Dandekar, D. P.; Randow, C.; Robinette, J. Shock Response of Polyurea; U.S. Army Research Laboratory: Aberdeen Proving Ground, MD; unpublished data, 2011.

NO. OF
COPIES ORGANIZATION

1 (PDF) DEFENSE TECHNICAL INFORMATION CTR DTIC OCA

1 (PDF) DIRECTOR US ARMY RESEARCH LAB IMAL HRA

1 (PDF) DIRECTOR US ARMY RESEARCH LAB RDRL CIO LL

1 (PDF) GOVT PRINTG OFC A MALHOTRA

ABERDEEN PROVING GROUND

1 (PDF) DIR USARL RDRL WMP C D CASEM